Since January 2020 Elsevier has created a COVID-19 resource centre with free information in English and Mandarin on the novel coronavirus COVID-19. The COVID-19 resource centre is hosted on Elsevier Connect, the company's public news and information website.

BASIC SCIENCE

Nanomedicine: Nanotechnology, Biology, and Medicine
35 (2021) 102338

Original Article

nanomedjournal.com

A novel liposome-polymer hybrid nanoparticles delivering a multi-epitope self-replication DNA vaccine and its preliminary immune evaluation in experimental animals

Zhangting Zhao, MSe[a,1], Xingyuan Ma, PhD[a,1], Ruihuan Zhang, MSe[a], Fabiao Hu, PhD[a], Tong Zhang, MSm[b], Yuping Liu, MSm[b], Myong Hun Han, PhD[a,c], Fang You, PhD[d], Yi Yang, PhD[e,*], Wenyun Zheng, PhD[b,*]

[a]State Key Laboratory of Bioreactor Engineering, East China University of Science and Technology, Shanghai, PR China
[b]Shanghai Key Laboratory of New Drug Design, School of Pharmacy, East China University of Science and Technology, Shanghai, PR China
[c]Department of Genetics, Faculty of Life Science, KIM IL SUNG University, Pyongyang, Democratic People's Republic of Korea
[d]Department of Chemical and Biomolecular Engineering, National University of Singapore, Singapore 117585, Singapore
[e]SinGENE Biotech Pte Ltd, Singapore Science Park, Singapore 118258, Singapore

Revised 6 October 2020

Abstract

DNA vaccine is an attractive immune platform for the prevention and treatment of infectious diseases, but existing disadvantages limit its use in preclinical and clinical assays, such as weak immunogenicity and short half-life. Here, we reported a novel liposome-polymer hybrid nanoparticles (pSFV-MEG/LNPs) consisting of a biodegradable core (mPEG-PLGA) and a hydrophilic shell (lecithin/PEG-DSPE-Mal 2000) for delivering a multi-epitope self-replication DNA vaccine (pSFV-MEG). The pSFV-MEG/LNPs with optimal particle size (161.61 ± 15.63 nm) and high encapsulation efficiency (87.60 ± 8.73%) induced a strong humoral (3.22-fold) and cellular immune responses (1.60-fold) compared to PBS. Besides, the humoral and cellular immune responses of pSFV-MEG/LNPs were 1.58- and 1.05-fold than that of pSFV-MEG. All results confirmed that LNPs was a very promising tool to enhance the humoral and cellular immune responses of pSFV-MEG. In addition, the rational design and delivery platform can be used for the development of DNA vaccines for other infectious diseases.

Key words: DNA vaccine; Liposome-polymer hybrid nanoparticles; Delivery; Immune evaluation; Infectious diseases

Infectious diseases are caused by living pathogenic microorganisms including viruses, bacteria, and fungi. These diseases can be transmitted, directly or indirectly, from person to person by contact. According to the World Health Organization (WHO), 3 infectious diseases are ranked in the top 10 causes of death worldwide in 2016, including lower respiratory infections (3.0 million deaths), diarrheal diseases (1.4 million deaths), and tuberculosis (1.3 million deaths).[1] Thus far, more than 10 million confirmed cases and almost half million deaths worldwide have been reported due to the coronavirus disease (COVID-19) pandemic.[2] Given that infectious diseases are a significant threat to public health and the global economy, significant progress has been made in infectious disease management. Since the 1940s, antibiotics have saved millions of lives and play a critical role in the treatment and prevention of various infectious diseases.[3] However, though powerful, antibiotics only work for the bad bacterial infections but not for viral infections. What's worse, after decades of misuse and overuse of antibiotic, they are becoming less effective and has led to the emergence of "superbugs", which are also known as antimicrobial resistance bacteria (ARB).[4] In recent years, the rise and spread of ARB is building up to become an epic global public health crisis.

Funding Source: This work was supported by the National Key Research and Development Project of China (2018YFA0902804), the National Natural Science Foundation (31670944, 81673345), and the Science and Technology Innovation Action Plan of Shanghai (17431904600).
Disclosure: The authors of this article declare no conflicts of interest.
* Corresponding authors.
E-mail addresses: yangyi@singenebio.com (Y. Yang), zwy@ecust.edu.edu.cn (W. Zheng).
[1] These authors contributed equally to this work.

https://doi.org/10.1016/j.nano.2020.102338
1549-9634/

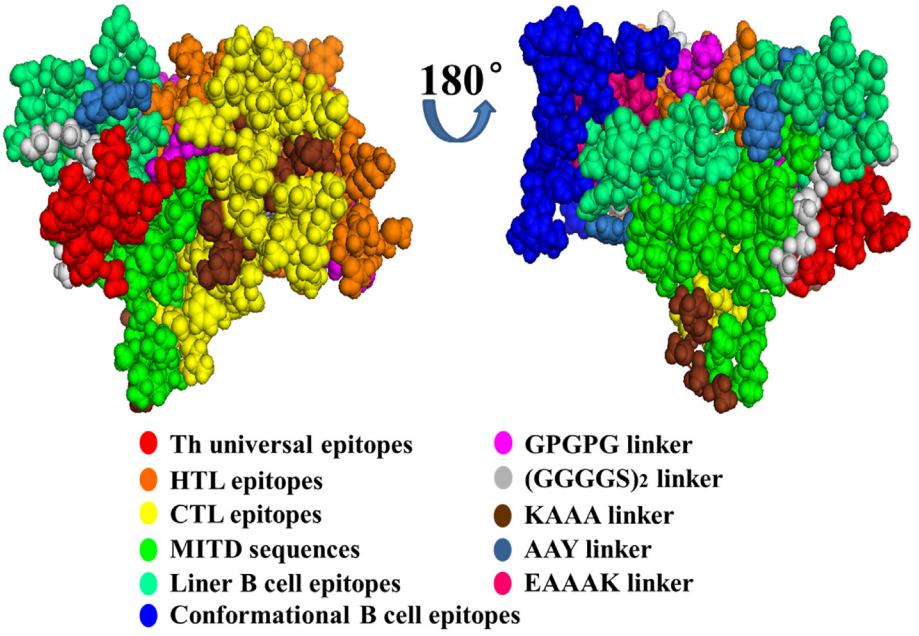

Figure 1. Three-dimensional structure simulation and analysis of MEG by online software I-TASSER.

Vaccination, on the other hand, is one of the major success stories of modern medicine which effectively prevents and eradicates many infectious diseases, both viral and bacterial.[5] Different from antibiotics, which are used to kill the bacteria causing the infection, vaccinations boost the body's immune system by stimulating the production of antibodies. Conventional vaccine approaches, which use either entire pathogens (whole-cell vaccines) or a fragment of a pathogen (subunit vaccines) to stimulate the immune responses, though successful in certain cases, suffer from many shortcomings such as severe side effects, hard to manipulate, and lack of protective mucosal immunity.[6]

Recently, nucleic acid vaccine, as a new type of vaccine has emerged, which offers several unique advantages over the traditional vaccines. Firstly, nucleic acid vaccine is a relatively cheaper and safer approach as it consists of only the DNA or RNA sequence, which is taken up and translated into antigen(s) by host cells. Secondly, nucleic acid vaccine is highly focused as the immune responses are directed toward only the selected antigen(s) of interest. Besides, nucleic acid vaccine is highly effective as it mimic the active infection by expressing antigens *in situ*, thereby priming both B- and T- cell responses. Furthermore, nucleic acid vaccine provides a rapid response platform which capable of producing protective vaccine in a short time-frame.[5,7–9] Unfortunately, thus far development for RNA vaccination is limited by the fact that RNA is relatively unstable *in vivo*. Other challenges, including unintended immune reaction, difficulty and expense of large-scale RNA production render the RNA vaccines are still under development and evaluation.[10,11] However, DNA vaccines have been approved for veterinary use.[12] Now, the global COVID-19 pandemic has made the field of DNA vaccines developing rapidly; candidates from Scancell, Inovio and CanSino Bio all reported at the early-stage of human clinical trials.[13–16] DNA vaccination can overcome most limitations of conventional vaccines, still, there are two main technical challenges hinder the development of DNA vaccines from trial to market: 1) the lacking of methods to identify the most effective DNA-encoding antigens that can elicit the best immune response; 2) the absence of appropriate strategy to induce a strong, stable, and long-lasting immune response.[7,17]

We are interested in developing a novel DNA vaccine platform which can deliver potent and long-term immune response for infectious diseases. In the current study, we firstly reported an efficient multi-epitope self-replication DNA vaccine with a new liposome-polymer hybrid nanoparticles (LNPs) delivery system (Figure 1). DNA vaccine was rationally designed based on the optimal B- and T-cell epitopes and linkers; and the LNPs were fabricated with two key components, a biodegradable core and a hydrophilic shell. *In vitro* and *in vivo* results showed that the new type multi-epitope self-replication DNA vaccine encapsulated in LNPs was stable and induced strong humoral and cellular immune responses. Our newly developed strategy is a versatile platform for other DNA vaccine design and delivery and has the potential to be applied for the prevention and treatment of other diseases.

Methods

Materials

Poly[(ethylene glycol)-*co*-(D, L-lactide-*co*-glycolide)] (mPEG-PLGA) was taken from Jinan Daigang Biomaterial Co., LTD (Shandong, China). Lecithin and 1,2-distearoyl-sn-glycero-3-phosphoethanolamine-N-[maleimide(polyethylene-glycol)-2000] (PEG-DSPE-Mal 2000) were commercially available from A.V.T. pharmaceutical technology co., LTD (Shanghai, China). Plasmid DNA extraction kit was purchased from Majorbio co., LTD (Shanghai, China). His tag mouse monoclonal antibody diluent, goat anti-mouse AlexaFluor 488®,

Table 1
Bioinformatics tools used for the rational design of multi-epitope DNA vaccines.

Prediction tools	Function	Accuracy /AUC/R2	Website
ABCpred	Linear B-cell epitopes	65.93%	http://crdd.osdd.net/raghava/abcpred/
Bcepred	Linear B-cell epitopes	0.8	http://ailab.ist.psu.edu/bcpred/predict.htm
DiscoTope2.0	Conformational B-cell epitopes	0.73	https://www.cbs.dtu.dk/services/DiscoTope/
ElliPro	conformational B-cell epitopes	NA	https://tools.iedb.org/ellipro/
NetMHCpan 4.0	HLA class I epitope HLA class II epitope	NA	http://www.cbs.dtu.dk/services/NetMHCpan/
IEDB	HLA class I epitope HLA class II epitope	0.86 0.85	https://tools.iedb.org/mhci/ https://tools.iedb.org/mhcii/
RANKPEP	MHC I	NA	http://bio.dfci.harvard.edu/RANKPEP/
CTLPred	MHC I	75.8%	http://crdd.osdd.net/raghava/ctlpred/index.htmL
PAComplex	MHC I MHC II	NA	http://pacomplex.life.nctu.edu.tw./
I-TASSER	Automatic protein structure prediction	NA	https://zhanglab.ccmb.med.umich.edu/I-TASSER/
PROCHECK	Stereochemical quality of a protein structure	NA	https://servicesn.mbi.ucla.edu/PROCHECK/
Prosa	Recognize the potential errors	NA	https://prosa.services.came.sbg.ac.at/prosa_.php
ProtParam	Grand average of hydropathicity	NA	https://web.expasy.org/protparam/
VaxiJen	Protein antigenicity	78.00%	https://www.ddg-pharmfac.net/vaxijen/VaxiJen/VaxiJen.htm

The main online bioinformatics software was used in this study. NA represented not analyzed.

3-(4, 5-dimethylthiazol-2-yl)-2, 5-diphenyltetrazolium bromide (MTT), and Hoechst 33342 were purchased from Beyotime (Shanghai, China). The mouse IgG total ready-set-go kit, FITC anti-mouse CD4 antibody, and APC anti-mouse CD8α antibody were purchased from Biolegend (California, USA). All other reagents used in this study were of analytical grade. Normal liver L-02 cells were acquired from the Type Culture Collection Committee of Chinese Academy of Sciences (Shanghai, China). Fetal bovine serum (FBS), Dulbecco's Modified Eagle Medium (DMEM), and penicillin–streptomycin (10,000 U/mL penicillin and 10 mg/mL streptomycin) were obtained from Thermo Fisher Scientific (Waltham, USA).

Selection of antigen epitopes to design multi-epitope DNA vaccine

Heat-labile-enterotoxin B (LTB), colonization factor antigen-I (CFA/I), CFA/IV surface antigen 6 (CS6), and invasive plasmid antigen B (IpaB) are the main antigens in ETEC and *Shigella* that cause traveler's diarrhea (TD).[18–21] The protein sequences of LTB, CFA/I, CS6, and IpaB were obtained from the PDB database. The linear B-cell epitopes were analyzed by ABCpred and Bcepred, while the conformational B-cell epitopes were predicted by DiscoTope 2.0 and ElliPro. T-cell epitopes were restricted by major histocompatibility complex (MHC) and classified into 2 types, MHCI and MHCII. Helper T lymphocytes (HTL) and cytotoxic lymphocyte (CTL) belongs to MHCI and MHCII, respectively[22], which were respectively analyzed by NetMHCpan 4.0 and IEDB. Besides, both T-cell epitopes were evaluated by RANKPEP. Similarly, the modest CTL epitopes candidates were predicted by CTLPred and PAComplex. The selected 16 B- and T-cell epitopes had super-hydrophilicity, excellent flexibility, high accessibility, and strong antigenicity, and needed MHC restriction (Table 2).

Design, evaluation, and construction of candidate DNA vaccine

On the basis of the alphavirus vector pSFV1, the SP6 promoter of pSFV1 was replaced by the dual promoter CMV/T7 by overlap extension PCR, which was named pSFV. A series of linker peptides ($(GGGGS)_2$, GPGPG, KAAA, AAY, and EAAAK) were used to connect different types epitopes to ensure the independence and integrity of each epitope and improve the efficiency of epitope recognition (Figure S3A). Besides, the universal Th epitopes and MHCI trafficking domain (MITD) sequences were introduced at the N- and C-terminal of T-cell epitopes respectively to reduce the MHC polymorphism and improve the efficiency of epitopes presentation and recognition (Figure S3A).[23] The quality of the designed MEG was accessed by I-TASSER, DNAStar, and PROCHECK, respectively. Besides, the immunogenicity and proteasome cleavage site of the MEG were analyzed by PAProC and the overall antigenicity of MEG was evaluated by VaxiJen 2.0 (with a 0.4 threshold). All the online bioinformatic softwares used in this study were listed in Table 1.

In addition, Kozak sequence (GCCGCC) and His tags were respectively added before and after MEG sequences. Codon optimization and gene synthesis were performed by Reidi Biotechnology co., LTD (Shanghai, China) to improve the expression level of MEG antigen in mammalian cell. Two high-level expression vectors (pcDNA3.1 and pSFV) were selected to construct 5 recombinant plasmids (pSFV, pcDNA3.1-MEG, pSFV-MEG, pcDNA3.1-MEG-EGFP (green fluorescent protein), and pSFV-MEG-EGFP) (Figure S3B). All primers used in this study were listed in Table S1.

Preparation of DNA-loaded LNPs

LNPs were prepared through a modified nanoprecipitation method (Figure S4).[24] First, 6 mg of mPEG-PLGA and 50 μg of plasmid DNA (pcDNA3.1, pSFV, pcDNA3.1-MEG, pSFV-MEG, pcDNA3.1-MEG-EGFP, or pSFV-MEG-EGFP) were dissolved in 3 mL of ethyl acetate and shaken to form an emulsion (organic phase). Meanwhile, 0.84 mg of lecithin and 0.36 mg of PEG-DSPE-Mal 2000 were dissolved in 9 mL of 4% ethanol solution (molar ratio of 9: 1) (water phase). The aqueous

Table 2
The sequences of the screened antigen epitopes.

Major antigen	Epitope position	Sequence	Epitope type
LTB	1–24 aa	MNKVKCYVLFTALLSSLYAHGAPQ	HTL
	29–36 aa	ESMAGKRE	B (conformational)
	39–49 aa	VPGSQHIDSQK	B (linear)
	52–62 aa	YTINDKILSYT	CTL
CFA/I	23–31 aa	ADKNPGSEN	B (linear)
	43–56 aa	GSSPIYNILNSYLT	HTL
	253–263 aa	RFQDDNSKSDG	B (conformational)
	316–325 aa	TMPEISVPVLC	CTL
CS6	53–72 aa	MKKTIGLILILASFGSHARTEI	HTL
	91–99 aa	GAEVTPNQQ	B (conformational)
	106–118 aa	KEGGLLFSVSLTV	CTL
	141–151 aa	NYTSGIPPGIYN	B (linear)
IpaB	166–181 aa	LSELDPESPEKKKLSR	B (conformational)
	251–262 aa	QLMATFIQLVGK	HTL
	281–296 aa	SRKTEMERKSDEYAAE	B (linear)
	312–332 aa	KILGALLTIVSVVAAAFSGGA	CTL

phase was preliminarily heating to 65–70 °C; then, the organic phase solution was added dropwise (1 mL/min) to the preheated water phase under slow stirring. After that, the mixture was vortexed vigorously for 3 min, and slowly stirred at 25 °C for 2 h to evaporate the organic phase. The obtained nanoemulsion was concentrated with a 100 KDa ultrafiltration tube (Millipore, USA) and washed twice with ultrapure water to remove unencapsulated DNA. Finally, the DNA-loaded LNPs was frozen and saved at 4 °C. DNA-loaded mPEG-PLGA NPs and PLGA NPs were prepared as the same method.

Cell culture

L-02 cells were cultured in DMEM medium supplemented with 10% FBS and 1% penicillin–streptomycin at 37 °C with 5% CO_2. When the confluence reached 80–90%, cells were trypsinized and seeded into 24-well plates for each experiment.

Encapsulation efficiency of DNA-loaded LNPs

The concentration of DNA in the supernatant of LNPs was determined by an ultra-micro nucleic acid detector (Quawell, USA). All samples were performed in triplicate. Encapsulation efficiency (EE) was calculated using the Eq. (1) shown below.

$$EE\% = \frac{\text{Initial amount of DNA added} - \text{Amount of DNA in supernatant}}{\text{Initial amount of DNA added}} \times 100\% \quad (1)$$

Size and zeta potential of LNPs

The freeze-dried LNPs (1 mg) were resuspended in deionized water (10 mL) and dispersed by ultrasound. The samples were suspended in copper grids and dried and the morphology was observed by JEM-1400 transmission electron microscopy (TEM) (JEOL, Japan). The zeta potential and particle size of LNPs were measured and calculated by dynamic light scattering (DLS) (Malvern, UK) at 25 °C. Each sample was measured in triplicate.

Gel retardant experiments

The protective effect of LNPs on pSFV-MEG were evaluated by agarose gel electrophoresis. Naked pSFV-MEG and pSFV-MEG/LNPs incubated with DNase at 25 °C for 30 min, and then all samples were analyzed by agarose gel. The gray value of the electrophoretic band was quantified by Image J software (National Institutes of Health, USA).

In vitro DNA release and stability

The release profile of pSFV-MEG from LNPs, mPEG-PLGA NPs, and PLGA NPs were assessed in phosphate buffer solution (PBS, pH 7.4). The freeze-dried samples (1 mg) were dissolved in PBS (1 mL) and shaken in a shaker incubator (100 rpm, 37 °C). At specified times (0, 2, 4, 8, 24, 48, 72, and 96 h), the supernatant was collected and the test tube was carried forward to the release studies by adding 1 mL of fresh PBS. The DNA concentration in the supernatant was measured by an ultra-micro nucleic acid detector, and the *in vitro* release rate of DNA was calculated using the Eq. (1).

The stability of dried pSFV-MEG/LNPs was evaluated by particle size and encapsulation efficiency after 3- and 7- week storage at 4 °C and 25 °C, respectively.

Cytotoxicity assay

MTT assay was performed *in vitro* to determine the cytotoxicity of DNA-loaded LNPs. L-02 cells (6×10^4 cells/well) were seeded in 96-well plates and cultured overnight, and incubated with pcDNA3.1/LNPs, pcDNA3.1-MEG/LNPs, and pSFV-MEG/LNPs (equivalent DNA concentrations: 10, 20, 40, 80, and 100 μg/mL) for 24 and 48 h. Then, 20 μL of MTT (5 mg/mL) was added and continue incubated for another 4 h. The culture supernatant was discarded and 150 μL of DMSO was added to dissolve the precipitated crystals. The OD_{490nm} value was measured to calculate the cell viability.

Table 3
Characteristic parameters of pSFV-MEG/LNPs.

Samples	Particle size (nm)	PDI	Zeta potential (mV)	EE (%)
Blank LNPs	175.60 ± 26.79	0.142 ± 0.013	−17.5 ± 0.4	/
pSFV-MEG/LNPs	191.90 ± 38.16	0.125 ± 0.009	−29.3 ± 0.3	87.60 ± 8.73

Data were expressed as mean ± SD (n = 3).

Hemolysis assay

The red blood cells (RBC) were collected from BALB/C mice by centrifugation and diluted 10-fold with PBS containing 25 U/mL of heparin. The diluted RBC suspension (200 μL) was mixed with 800 μL of LNPs, pcDNA3.1-MEG/LNPs, and pSFV-MEG/LNPs (equivalent DNA concentrations: 10, 20, 40, 80, and 100 μg/mL) as experimental groups. In addition, 800 μL of PBS and ultrapure water were used as negative and positive control groups, respectively. The mixtures were incubated for 3 h at 37 °C and the supernatant were collected. The absorbance of hemoglobin in the supernatant was measured by UV–Vis spectrophotometer at 541 nm, and the hemolysis rate (HR) was calculated by the following formulas.

$$\mathrm{HR}\ (\%) = (\mathrm{OD_t}-\mathrm{OD_n})/(\mathrm{OD_p}-\mathrm{OD_n}) \times 100\% \quad (2)$$

Wherein, OD_t represents the absorbance values of experimental groups, and OD_n and OD_p are the absorbance values of negative and positive control, respectively.

Transfection efficiency

L-02 cells were transfected with Lipofectamine3000 (ThermoFisher Scientific, USA) according to manufacturer's protocols. Briefly, L-02 cells (2×10^5 cells/well) were seeded into 24-well plates to reach 70–90% cell confluences. Medium containing pcDNA3.1-MEG, pSFV-MEG, pcDNA3.1-MEG/LNPs, pSFV-MEG/LNPs, pcDNA3.1-MEG/Lipofectamine, and pSFV-MEG/Lipofectamine (500 ng) were added to each well for transfection. The transfection experiments were conducted in triplicates. Fluorescence signal was detected by flow cytometry with FITC channel (excitation: 488 nm and emission: 525 nm) after 48 h incubation.

Immunofluorescence detection

L-02 cells (2×10^5 cells/well) were seeded in 24-well plates and fixed with 4% paraformaldehyde after washing twice with PBS. After that, cells were incubated with 0.1% Triton X-100 for 10 min and 3% BSA for 1 h. Cells were then sequentially incubated with His-tagged mouse monoclonal antibody, goat anti-mouse AlexaFluor 488®, and Hoechst 33342 in the dark. Finally, the intracellular fluorescence was observed by invert fluorescence microscopy (Olympus, Japan).

Western blotting

Western blotting was used to test the expression of MEG antigen in L-02 cells. Proteins (50 μg) were separated by 12% SDS-PAGE electrophoresis and the band on the gel was electro-transferred onto the pretreated PVDF membranes (Beyotime Biotechnology, China). Subsequently, the PVDF membranes were blocked with 5% non-fat milk in Tris-buffer saline with Tween 20 for 1 h at 25 °C, and then incubated with anti-His tagged antibodies at 4 °C overnight and horseradish peroxidase (HRP)-labeled goat anti-mouse secondary antibody (Proteintech, USA) for 1 h at 25 °C. Protein bands were visualized with the ultrasensitive ECL chemiluminescence kit (Sangon Biotech, China). The gray values of the protein bands were analyzed by Image J.

Immunization plan

BALB/C mice used in the experiments were purchased from Leagene Biotechnology co., LTD (Shanghai, China). All animal procedures were performed in accordance with Chinese legislation on the Use and Care of Research Animals (Document No. 55, 2001), and the Guidelines for Care and Use of Laboratory Animals of East China University of Science and Technology University and experiments were approved by the Animal Ethics Committee of East China University of Science and Technology. Female BALB/C were randomly divided into 8 groups and administrated with PBS, bank LNPs, pcDNA3.1/LNPs, pSFV/LNPs, pcDNA3.1-MEG, pSFV-MEG, pcDNA3.1-MEG/LNPs, and pSFV-MEG/LNPs by intramuscular injection, respectively. The body weight of BALB/C mice was recorded at a fixed time every 3 days during the whole experiment. Each group was boosted on day 13-post and 26-post primary immunization. Blood samples were collected from the posterior orbital venous plexus on day 0, 14, 28, and 35 of mice. Serum was separated after centrifugation at 1000 rpm for 15 min and stored at −80 °C. On day 35, mice were sacrificed to collect their spleens for preparing spleen cells.

Serum antibody measurements

IgG antibodies were measured in serum samples by ELISA with the mouse IgG total ready-set-go kit. Briefly, 100 μL of capture antibody solution was added to Corning™ Costar™ 9018 ELISA plate (Corning, America). After incubation overnight at 4 °C, plates were washed twice and incubated with 250 μL of sealing buffer at 25 °C for 2 h. Assay Buffer A (1 ×) solution were respectively added to the blank (100 μL) and sample wells (90 μL) after 3 times washing. After that, pre-diluted serum or plasma samples (10 μL) and diluted detection antibody (50 μL) were added to each well in turn. The plates were sealed and incubated at 25 °C for 2 h with gently shaking and continue incubation at 25 °C for 15 min after adding substrate solutions (100 μL) to each well. The reaction was stopped with peroxidase-labeled secondary antibodies were developed with 3,3′,5,5-tetramethylbenzidine (TMB) substrate

(100 μL) for 15 min at 25 °C and the absorbance at 450 nm was measured on a microplate reader.

Distribution of T lymphocyte subsets in spleen

Individual samples of RBC-lysed spleen cells were filtered through a cell strainer (Becton, USA) to remove debris. The cells suspension (2×10^6 cells/well) was added to 96-well plates and incubated with FITC anti-mouse CD4 antibody and APC anti-mouse CD8α antibodies at 25 °C for 20 min in the dark, respectively. Then, 200 μL PBS was added to resuspend the cells after centrifugation. PBS was added as blank group. Cell fluorescence was detected by flow cytometry with FITC channel (excitation: 488 nm and emission: 525 nm) and APC channel (excitation: 650 nm and emission: 660 nm).

Evaluation of the toxicity of DNA-loaded LNPs in vivo

The major organs (heart, liver, spleen, lung, and kidney) of mice treated with PBS, pcDNA3.1-MEG/LNPs, and pSFV-MEG/LNPs were collected and fixed with 4% paraformaldehyde for paraffin slicing, followed by hematoxylin–eosin (HE) staining for histological examination.

Statistical analysis

All experiments were performed at least 3 times and results were expressed as mean ± standard deviation (SD). Statistical analysis of the data was performed by SPSS 22.0 software (IBM, USA). $P < 0.05$ was considered to be statistically significant.

Results

Rational design of multi-epitope DNA vaccine MEG

Several critical factors were taken into consideration in the rational design of the MEG sequence. Firstly, the antigen sequences (LTB, CFA/I, CS6, and IpaB) were retrieved from the PDB protein database (Scheme S1) to screen the optimal epitopes. According to the comprehensive evaluation of the online tools, the optimal epitopes (HTL, CTL, linear B-cell, and conformational B-cell epitopes) of each antigen with the highest score were chosen for the further studies (Table 1 and Table S1). Secondly, to enable efficient and stable expression of fusion proteins and also ensure the independence of functional epitopes, several linkers included HTL (GPGPG linker), CTL (KAAA linker), linear B-cell (AAY linker), and conformational B-cell (EAAAK linker) were selected to unite the same epitopes. Moreover, different types of epitopes was joined by $(GGGGS)_2$ linker to ensure the independence and integrity.[25–28] Thirdly, T-cell epitopes were connected in series in front of linear B-cell epitopes, which could improve the expression efficiency of antigens.[29] Fourthly, since it was important to avoid the MHC polymorphism restriction and improve the efficiency of epitope presentation and recognition, the universal Th epitope and MITD sequence were introduced at the N- and C-terminal of T-cell epitopes, respectively.[30] Finally, the corresponding tertiary structures were obtained by simulating the arranged MEG sequence with the three-dimensional (3D) simulation software I-TASSER, which could automatically generate high-quality model predictions of 3D structure and biological function of protein molecules from their amino acid sequences. Five different tertiary structures were successfully obtained (C-score within −5 to 2), and their corresponding C-scores were −1.08, −1.69, −2.66, −2.57, and − 4.33 (Figure S2), respectively. Due to the first 3D structure has the highest C-score value indicating high confidence, its corresponding amino sequence (Figure S3A) was selected as the optimal MEG sequence. Besides, additional analysis showed that only 28.2% amino residues of the first structure had a positive normalized B factor (NBF) value, while the NFB value of the rest four structures were all positive (Figure S2). Since residues with higher NBF value than 0 indicated that the protein was structurally unstable, this result further confirmed that the first structure was the most suitable and could be used as a DNA vaccine candidate (Figure 1).

Evaluation of the structure of MEG

To verify the general and local quality of MEG antigen, Prosa and PROCHECK were used to analyze the predicted MEG tertiary structure. As shown in Figure 2A, the Prosa Z-score of MEG antigen was −4.05, which was perfectly within the range of scores typically found for native proteins of similar size. The Ramachandran plot showed that 76.1% and 16.2% of the residues located in the favored and allowed areas, respectively, whereas only 7.7% residues were in disallowed regions (Figure 2B). The results above demonstrated that the structure of MEG antigen had a very high resolution and good structural quality, and the steric atomic clashes among the residues were minimal. Besides, the instability index (II) of MEG obtained from the ProtParam tool was 38.85, which classified MEG antigen as stable. Furthermore, the overall quality score of MEG antigen from ERRAT was 90.68% (Figure 2C). All the above results revealed that the selected MEG antigen had a stable tertiary structure.

The secondary structural properties of MEG antigen were evaluated by PAProC tool and DNAstar. There were several proteasome cleavage sites in the sequence, but most of them appeared at the junction, making the designed MEG antigen not only retained the integrity of the cell epitopes but avoided unnecessary immune response caused by the emergence of new epitopes (Figure 3A). Besides, the B-cell epitope consisted of 43.7% helix and 56.3% random coil, which was consistent with the fact that B-cell epitopes most likely existed in the β-turns and random curls regions to be easily recognized by B cell receptor (Figure 3B). What's more, the B-cell epitopes were found to be composed of 80.4% hydrophilicity areas, 77.3% hydrophilic regions, 64.7% flexible regions, and 91.5% surface probability areas, respectively. However, 65.1% T-cell epitopes were located in the strongly hydrophobic region with a hydrophobic index of 2.25. These results suggested that B-cell epitopes had strong hydrophilicity, excellent flexibility, and high surface accessibility, whereas T-cell epitopes were mostly distributed in hydrophobic regions (Figure 3C-D).[22] Figure 3C showed that 58.5% residues of MEG antigen had an antigen index close to 1.7. The antigenicity probability of MEG antigen calculated by the VaxiJen 2.0 server was 1.13, which further demonstrated that the new developed MEG antigen had excellent antigenicity.

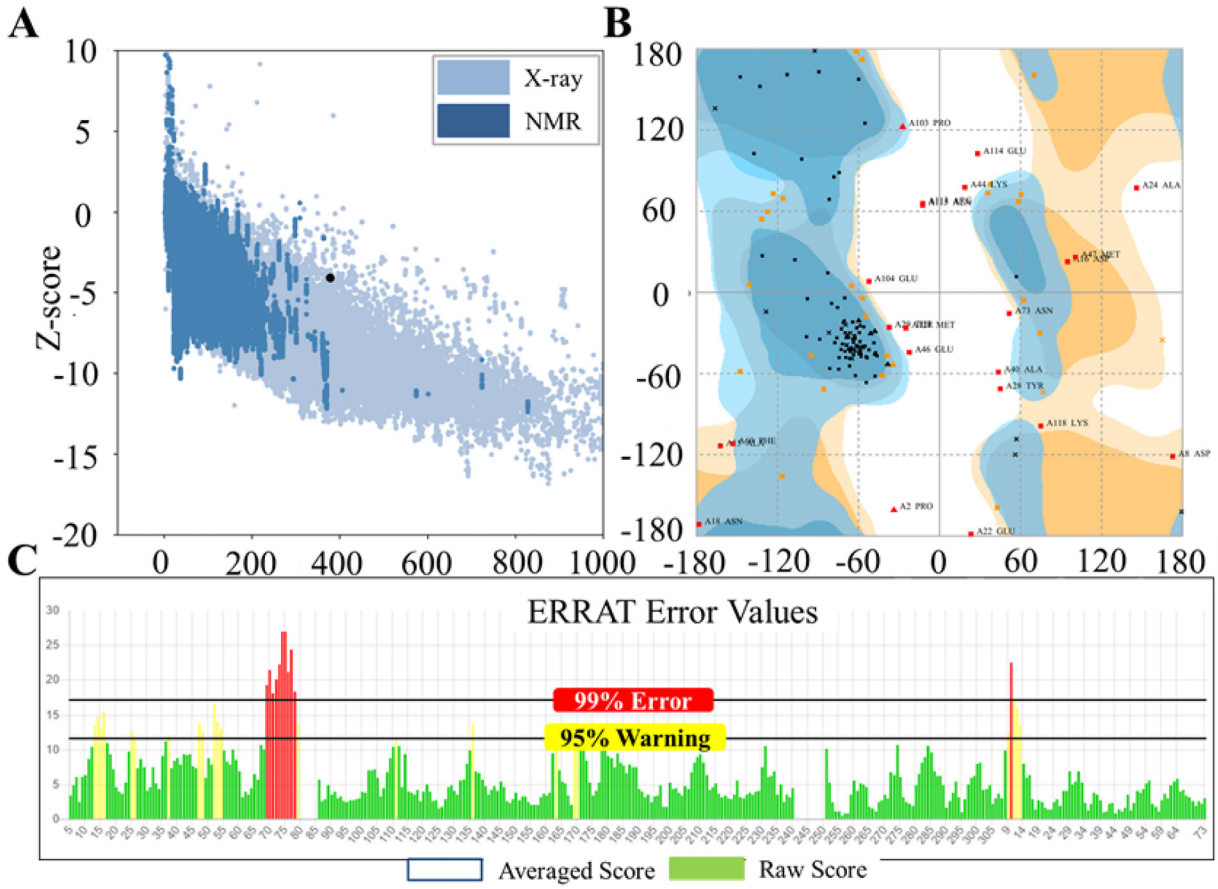

Figure 2. Tertiary structural validation of MEG. **(A)** The ProSA Z-score, **(B)** Ramachandran map, and **(C)** ERRAT plot of the MEG were evaluated.

Development of novel DNA-loaded LNPs

To evade the degradation and enhance the efficiency of DNA vaccine *in vivo*, a novel LNPs was developed through an improved single-step nanoprecipitation method. Biodegradable amphiphilic block copolymers mPEG-PLGA was used to encapsulate the DNA and form the core of LNPs; hydrophilic polymer PEG-DSPE-Mal 2000/lecithin was used as the shell of LNPs (Figure 4A). The molar ratio of lecithin and PEG-DSPE-Mal 2000 was very important in producing monodisperse LNPs with a best size range and high encapsulation efficiency. In the current study, a molar ratio of lecithin and PEG-DSPE-Mal 2000 from 6: 1 to 15: 1 was detected respectively, and finally 9:1 was identified to be the most optimal one. Under this condition, the encapsulation efficiency reached as high as 87.60 ± 8.73% (Figure S5), and the particle size was 161.61 ± 15.63 nm, which was favorable, as large particle (> 200 nm) could be cleared by RES.[31]

TEM and DLS were used to characterize the morphology and size of the LNPs. Both blank LNPs and pSFV-MEG/LNPs had excellent uniformity, sphere appearance, and their average particle size were 152.13 ± 15.30 nm and 161.61 ± 15.63 nm as detected by TEM, and 175.60 ± 26.79 nm and 191.90 ± 38.16 nm by DLS, respectively (Figure 4B). The size differences measured by TEM and DLS were due to the fact that TEM reflected the size of particles in a dry state while DLS in a liquid state (Figure 4D-E). Besides, the zeta potential of pSFV-MEG/LNPs was negative (−29.3 ± 0.3 mV) compared to blank LNPs (−17.5 ± 0.4 mV), which was attributed to DNA itself carried a large number of negative charges (Table 3).

Evaluation of novel DNA-loaded LNPs

To evaluate the performance of the newly developed LNPs, the encapsulation efficiency and release profile were investigated. Compared with mPEG-PLGA NPs (21.77 ± 2.18%) and PLGA NPs (43.33 ± 3.34%), the LNPs had the highest encapsulation efficiency (87.60 ± 8.73%), which was mainly attributed to the PEG-DSPE-Mal 2000/lecithin layer of LNPs could retain the encapsulated MEG, while the mPEG was buried inside the core of mPEG-PLGA NPs and PLGA NPs alone lacked a shell (Figure 5A). Besides, the encapsulated pSFV-MEG showed an excellent released pattern in LNPs, it could burst release about 40.59% within the first 8 h, but afterwards, the release rate become slower, and the cumulative release rate could reach 51.11% at 96 h. (Figure 5B). In contrast, more than half of pSFV-MEG was released from mPEG-PLGA NPs (51.72%) and PLGA NPs (78.26%) at 8 h, the cumulative release rate reached 96.23% and 96.15% at 96 h, respectively (Figure 5B). These results indicated that the PEG-DSPE-Mal 2000/lecithin shell played critical role in the molecular barrier, which helped the retention of DNA inside LNPs. This sustained release pattern was

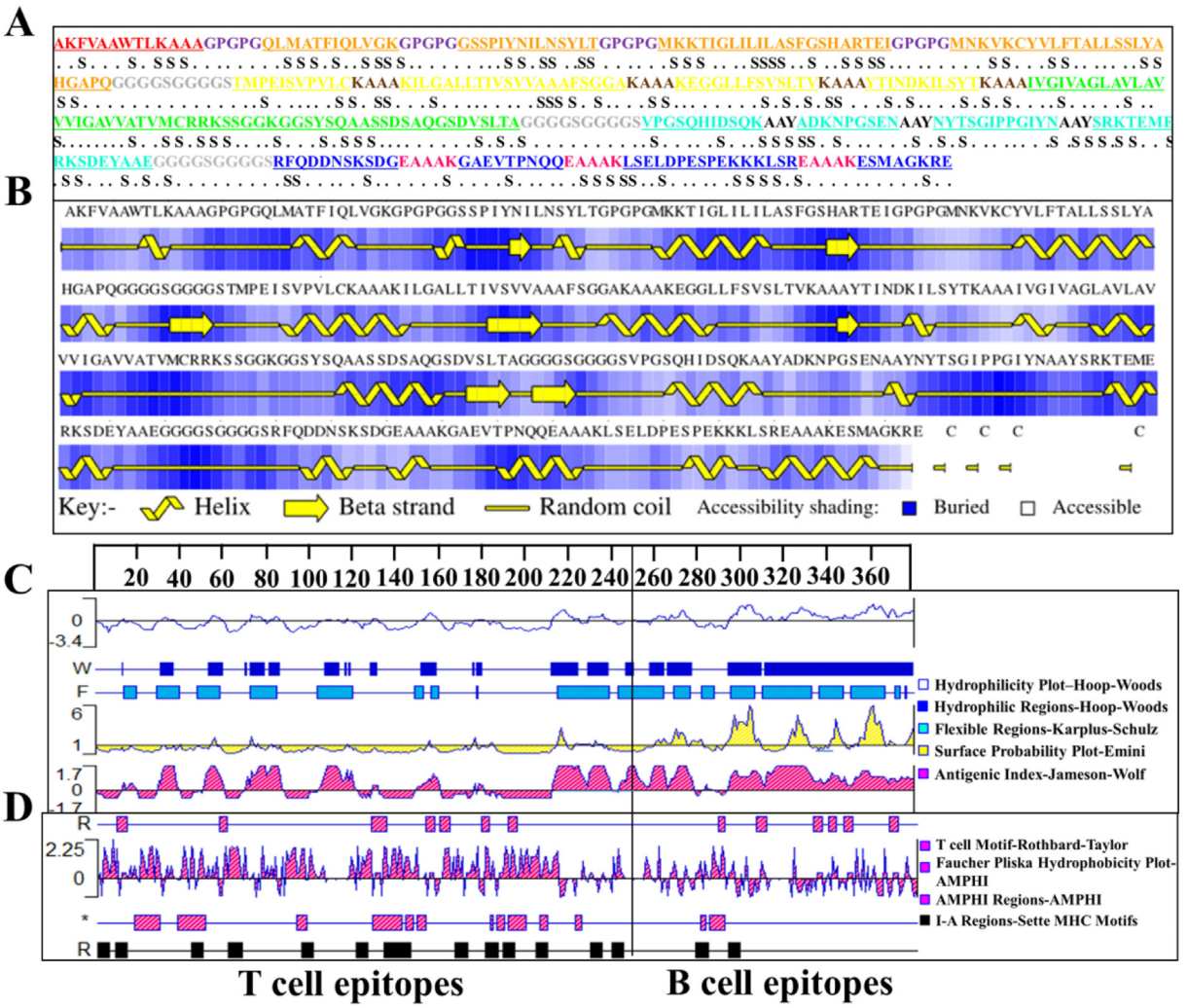

Figure 3. The immunogenicity analysis of MEG. **(A)** Proteasome cleavage sites in MEG predicted by PAProC software. **(B)** The secondary structure analysis of MEG. **(C)** The hydrophilicity, flexibility, surface accessibility, and antigen index of B- and T-cell epitopes of MEG was evaluated. **(D)** The T-cell epitopes of MEG was evaluated.

very important in therapy as it could improve the bioavailability and half-life of DNA vaccine *in vivo*, and also obtained a continuous immune response.

The protect effectiveness of the LNPs was evaluated through gel block experiment. The LNPs could well protect the encapsulated pSFV-MEG from degradation by DNase (Figure 5C and S5). Meanwhile, the stability test further showed that the prepared pSFV-MEG/LNPs was very stable, which could be stored at 4 °C or 25 °C for up to 7-week without any significant changes in encapsulation efficiency. The particles size of pSFV-MEG/LNPs also had little change at 4 °C, whereas it increased significantly at 25 °C (from 161.61 ± 15.63 nm to 210.09 ± 20.94 nm and 252.13 ± 26.38 nm at 3-week and 7-week, respectively) (Figure 5D). Therefore, the dried pSFV-MEG/LNPs could be storage at 4 °C at least for 7-week.

Cytotoxicity assay of DNA-loaded LNPs in vitro

MTT and hemolysis assay were performed to evaluate the cytotoxicity of LNPs. Figure 6A showed that after 24 h of incubation with blank LNPs, pcDNA3.1-MEG/LNPs, and pSFV-MEG/LNPs, the cell viability could still reach more than 90% even at the highest DNA concentration (100 μg/mL), and the high cell viability could be maintained for at least another 24 h without any significant difference (Figure 6B). These results indicated that blank LNPs or DNA-loaded LNPs had little cytotoxicity toward normal cells. Moreover, the highest concentrations of blank LNPs, pcDNA3.1-MEG/LNPs, or pSFV-MEG/LNPs hardly resulted in hemolysis of mice erythrocyte (less than 5%) after incubation at 37 °C for 3 h (Figure 6C), suggesting that the blank LNPs and DNA-loaded LNPs rarely caused cellular hemolysis. All the above results further reflected that LNPs were safe as a DNA vaccine carrier.

LNPs enhanced the expression of MEG antigen in L-02 cells

To explore the expression pattern of DNA-loaded LNPs, both naked DNA and DNA-loaded LNPs were transfected into L-02 cells, respectively. As shown in Figure 7A and S7, the transfection efficiency of pcDNA3.1-MEG/LNPs, pSFV-MEG/

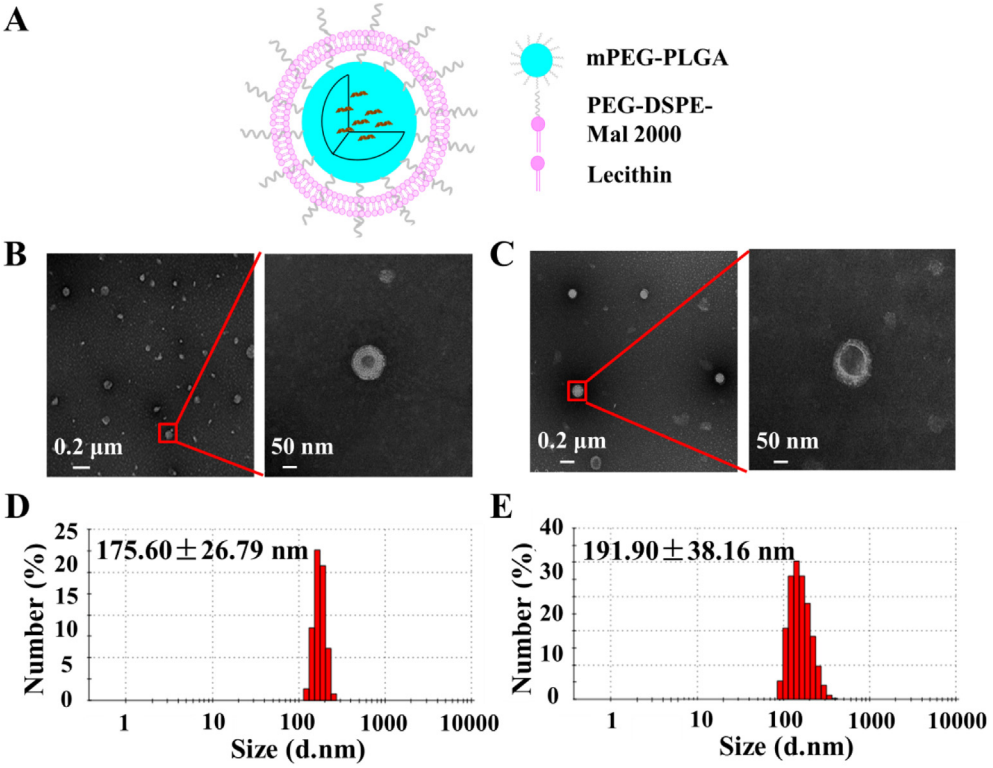

Figure 4. Preparation and characterization of pSFV-MEG/LNPs. **(A)** Structural diagram of pSFV-MEG/LNPs. The pSFV-MEG/LNPs comprised of a hydrophobic mPEG-PLGA core and a hydrophilic DSPE-PEG 2000/lecithin shell. The morphology of blank LNPs **(B)** and pSFV-MEG/LNPs **(C)** detected by TEM (Bar = 0.2 μm or 50 nm). Particle size of blank LNPs **(D)** and pSFV-MEG/LNPs **(E)** detected by DLS. Data were expressed as mean ± SD (n = 3).

LNPs, pcDNA3.1-MEG/Lipofectamine, and pSFV-MEG/Lipofectamine were 6.43-, 6.84-, 7.54-, and 8.19-fold and 5.17-, 5.50-, 6.04-, and 6.59-fold higher than that of blank pcDNA3.1-MEG and pSFV-MEG, respectively. Besides, the transfection efficiency of pcDNA3.1-MEG/LNPs (23.8%) and pSFV-MEG/LNPs (25.3%) were found without statistic difference to pcDNA3.1-MEG/Lipofectamine (27.9%) and pSFV-MEG/Lipofectamine (30.3%) (Figure 8A), which indicated that LNPs provided a comparable DNA transfection efficiency as Lipofectamine. Because the cell membrane was composed of phospholipid bilayers, the lecithin in LNPs could mediate the uptake of NPs by the cell *via* fusing with the cell membrane. Moreover, the expression of MEG antigen was detected in cells transfected with pcDNA3.1-MEG/LNPs and pSFV-MEG/LNPs by western blotting and immunofluorescence (Figure 7B-C). The gray values of pcDNA3.1-MEG/LNPs and pSFV-MEG/LNPs band were 0.85 and 0.88, respectively, which demonstrated that DNA-loaded LNPs expressed antigens adequately in mammalian cells.

Intramuscular administration of pSFV-MEG/LNPs induced robust immune responses to MEG

To evaluate the humoral immune response of pSFV-MEG/LNPs, the total amount of serum IgG antibodies of mice was detected by ELISA.[32] The fitting of the ELISA standard curve of IgG antibodies was shown in Figure S7. As presented in Figure 8A, the mice vaccinated with blank LNPs, pcDNA3.1/LNPs, pSFV/LNPs, pcDNA3.1-MEG/LNPs, and pSFV-MEG/LNPs showed detectable levels of serum total IgG anti-MEG after the boost immunization, and the antibodies in serum reached highest levels after the third immunization. The results showed that MEG could activate the humoral immune system of mice. The total amount of IgG antibodies in pcDNA3.1-MEG, pSFV-MEG, pcDNA3.1-MEG/LNPs, and pSFV-MEG/LNPs were 1.71-, 2.04-, 2.50-, and 3.22-fold higher than that of PBS group after the third immunization. Besides, MEG-loaded LNPs played a better role in inducing humoral immune response; and the total IgG levels in pSFV-MEG/LNPs and pcDNA3.1-MEG/LNPs were 1.58- and 1.46-fold high than pSFV-MEG and pcDNA3.1-MEG, suggesting that LNPs enhanced the humoral immune response. Interestingly, the total IgG levels in pSFV-MEG and pSFV-MEG/LNPs were 1.19- and 1.27-fold than that in pcDNA3.1-MEG and pcDNA3.1-MEG/LNPs, which indicated that pSFV plasmid as DNA vaccine vector had certain immune stimulation effect.

$CD4^+$ T cells are helper T lymphocytes, whose main function is to enhance the humoral immune response mediated by B cells. While $CD8^+$ T cells are inhibitory/lethal T lymphocytes, whose primary function is to specifically kill target cells directly.[33,34] The distribution of $CD4^+$ T and $CD8^+$ T cells in the spleen of mice was analyzed to examine the MEG-induced cellular response. As can be seen from Figure 8B and S9, there was no statistical difference of $CD8^+$ T cells in each group, but the $CD4^+$ T cells increased significantly after the third time immunization. Compared to the PBS group, the $CD4^+$ T cells in blank LNPs group increased 1.20-fold, demonstrating that LNPs alone

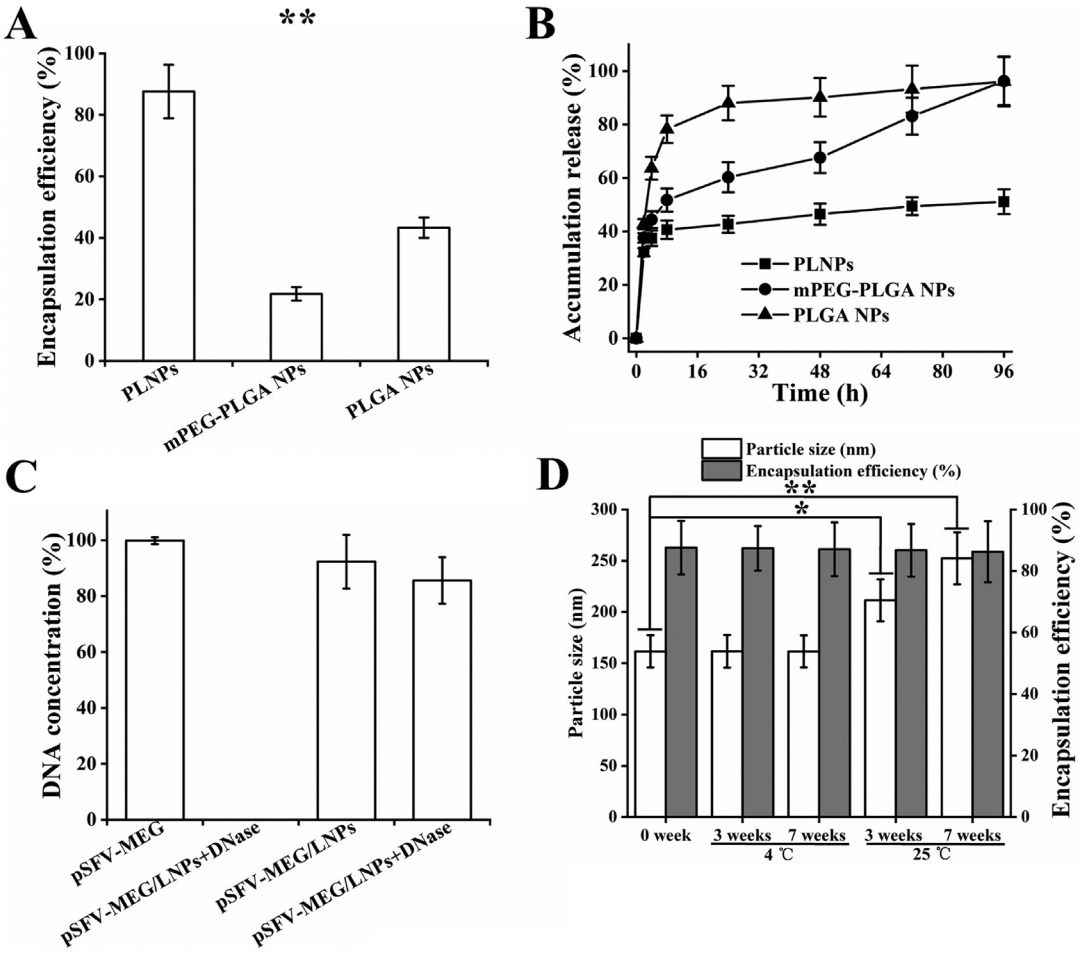

Figure 5. *In vitro* characteristic analysis of DNA-loaded LNPs. **(A)** The encapsulation efficiency of LNPs measured by an ultra-micro nucleic acid detector. **(B)** *In vitro* drug release from LNPs, mPEG-PLGA NPs, and PLGA NPs was evaluated in PBS (pH 7.4) at 37 °C. **(C)** Changes in particle size and EE of pSFV-MEG/LNPs at 4 °C and 25 °C for 3 weeks and 7 weeks. Data were expressed as mean ± SD (n = 3). $*P < 0.05$ and $**P < 0.01$.

enhanced the $CD4^+$ T cell immune response. Besides, the $CD4^+$ T cells in pSFV-MEG/LNPs group increased significantly among all groups, which was 1.60-fold higher than PBS group. The pSFV-MEG/LNPs induced a strong $CD4^+$ T cell immune responses (1.05-fold) compared to pSFV-MEG. Moreover, the $CD4^+$ T cell levels in pSFV-MEG and pSFV-MEG/LNPs groups were also higher than that in the pcDNA3.1-MEG and pcDNA3.1-MEG/LNPs groups (1.14- and 1.02-fold), which reconfirmed that the self-replication vector pSFV could enhance $CD4^+$ T cell immune response.

Biosafety evaluation of the LNPs in vivo

To evaluate the biosafety of different LNPs *in vivo*, the body weight of mice was monitored during the whole immunization experiment and the main organs (heart, liver, spleen, lung, and kidney) were collected for health evaluation. During the immunization period, the mice did not show any signs of discomfort and the body weight of mice treated with different LNPs increased regularly (Figure 9A). Besides, main organs were identified to be healthy after immunization regardless of types of reagents (LNPs or PBS) (Figure 9B). These results further demonstrated that the novel developed LNPs were safe enough for DNA vaccine delivery.

Discussion

As one of the most prevalent disease in low-income countries worldwide, TD infects 300 million people every year.[35] According to Intestinal Center Study, TD is mainly caused by two major pathogens, including *Enterotoxigenic Escherichia coli* and *Shigella*.[36] Although current antibiotics are critical treatment and prevention drugs for TD, they have been gradually denied because of the increasing number of ARB.[37] To the best of our knowledge, DNA vaccines have potential advantages compared to antibiotics and other traditional vaccines, which is easy to adapt to new and fast-emerging diseases by changing the antigen sequence.[6] Meanwhile, the advantages of multi-epitope DNA vaccines have been gradually discovered, especially with immunodominant B- and T-cell epitopes. Until now, the safety and effectiveness of multi-epitope DNA vaccines in human have been tested by many clinical trials, such as NCT02348320 and NCT02157051 for breast cancer, NCT02172911 for cervical

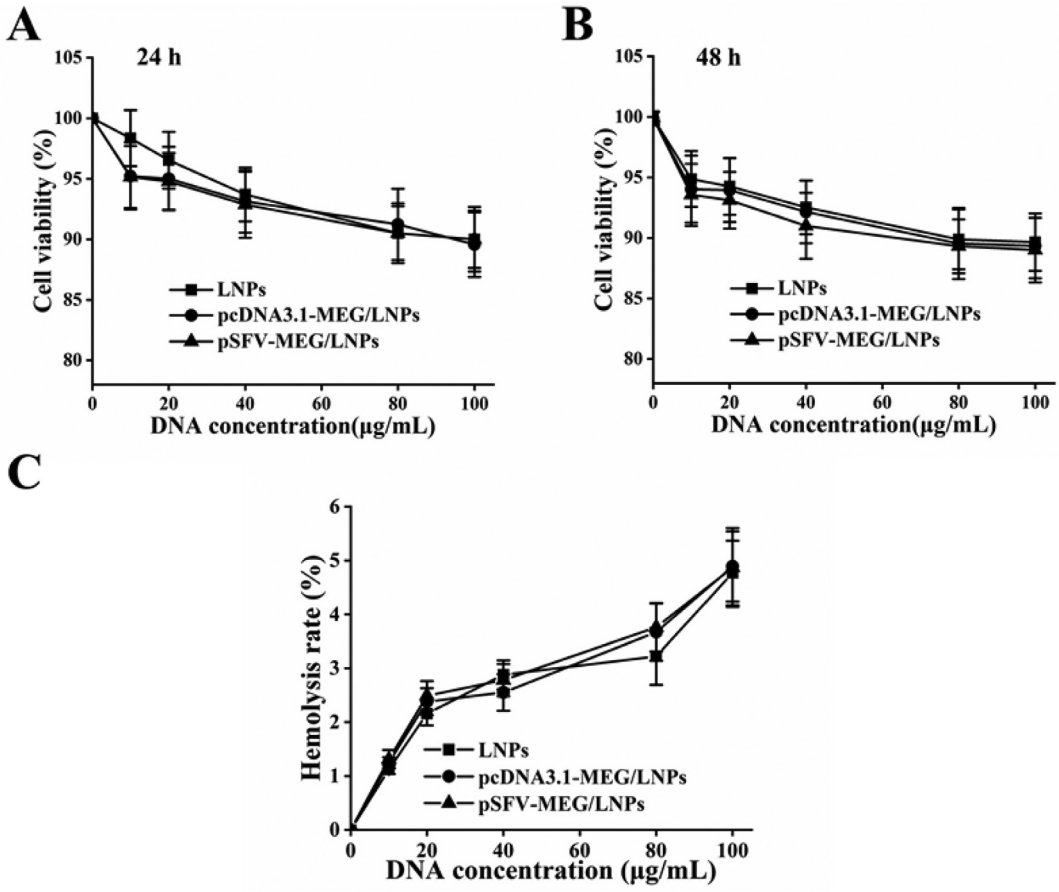

Figure 6. Cytotoxicity assay of pSFV-MEG/LNPs. The viabilities of L-02 cells treated with LNPs, pcDNA3.1-MEG/LNPs, and pSFV-MEG/LNPs for 24 h **(A)** and 48 h **(B)** were measured by MTT assay. **(C)** Hemolysis rate of mouse erythrocyte dispersion after incubation with different concentrations of LNPs at 37 °C for 3 h. Data were expressed as mean ± SD (n = 3). $*P < 0.05$, $**P < 0.01$, and $***P < 0.001$.

cancer.[8] However, low antigenicity and lack of stable delivery system limit the use of DNA vaccines.

Currently, several studies have reported that the design of multi-epitope DNA vaccines based on online softwares.[22,23] Partial protection in BALB/C mice had been seen, and the multi-epitope vaccines displayed suboptimal immunogenicity or weaker immune responses. Thus, we designed the multi-epitope DNA vaccine reasonably, and the design principles as follows: 1) active B- and T-cell epitopes to enhance immunogenicity; 2) leader sequence to enhance the stability of mRNA; 3) Kozak sequence and strong promoter to improve transfection efficiency in mammalian cells; 4) appropriate linker peptides to improve the immunogenicity; 5) codon optimization to improve expression level.[17] Study results showed that pSFV-MEG improved both humoral (1.19-fold) and cellular immunity (1.14-fold) compared to pcDNA3.1-MEG. Previous studies have shown that self-replication plasmid pSFV can enhance the immune response without integration into the genome.[38] Besides, the selected 16 epitopes based on online tools were consistent with clinically attenuated multivalent vaccines for TD.[39–41] The Z-score (−4.05) of MEG antigen was similar to the other reports.[12,42] Furthermore, the developed vaccine had an antigenicity probability of 1.13, which was higher than that in Gummow et al.[12] (0.48) and Pourseif et al.[35] (0.87) reports. The results indicated that MEG was high immunogenic compared to previously studies.

Although DNA vaccines are expected to be promising as a new *in vivo* vaccination platforms, the sustained delivery still poses a substantial challenge.[43] To protect DNA from DNase degradation and control release, different kinds of DNA delivery systems have also been developed, such as chitosan, PEI, PLGA, and liposomes.[6,44,45] Among them, PLGA and liposomes are the most promising and have been approved by the Food and Drug Administration (FDA) for medical applications.[24] However, the degradation of PLGA NPs can acidify the microenvironment, disrupt the dynamic balance, and hardly provide strong protection for DNA vaccines from enzymes. Also, there are several challenges that hinder the transition of liposomes to clinical research, including circulating instability and rapid clearance from the body.[6] Polyethylene glycol (PEG) is an FDA-approval polymer and commonly used for surface functionalization of NPs. The major function of PEG is to shield the surface charge of NPs and improve the half-life *in vivo*.[46] As previously reported, PEGylated-PLGA and lecithin NPs decrease uptake by RES, prolong blood residence, and well avoid the interaction with serum proteins.[47] LNPs combined the merits of liposomes and polymeric NPs have been widely studied for drug delivery. At the same time, the self-assembled LNPs have been

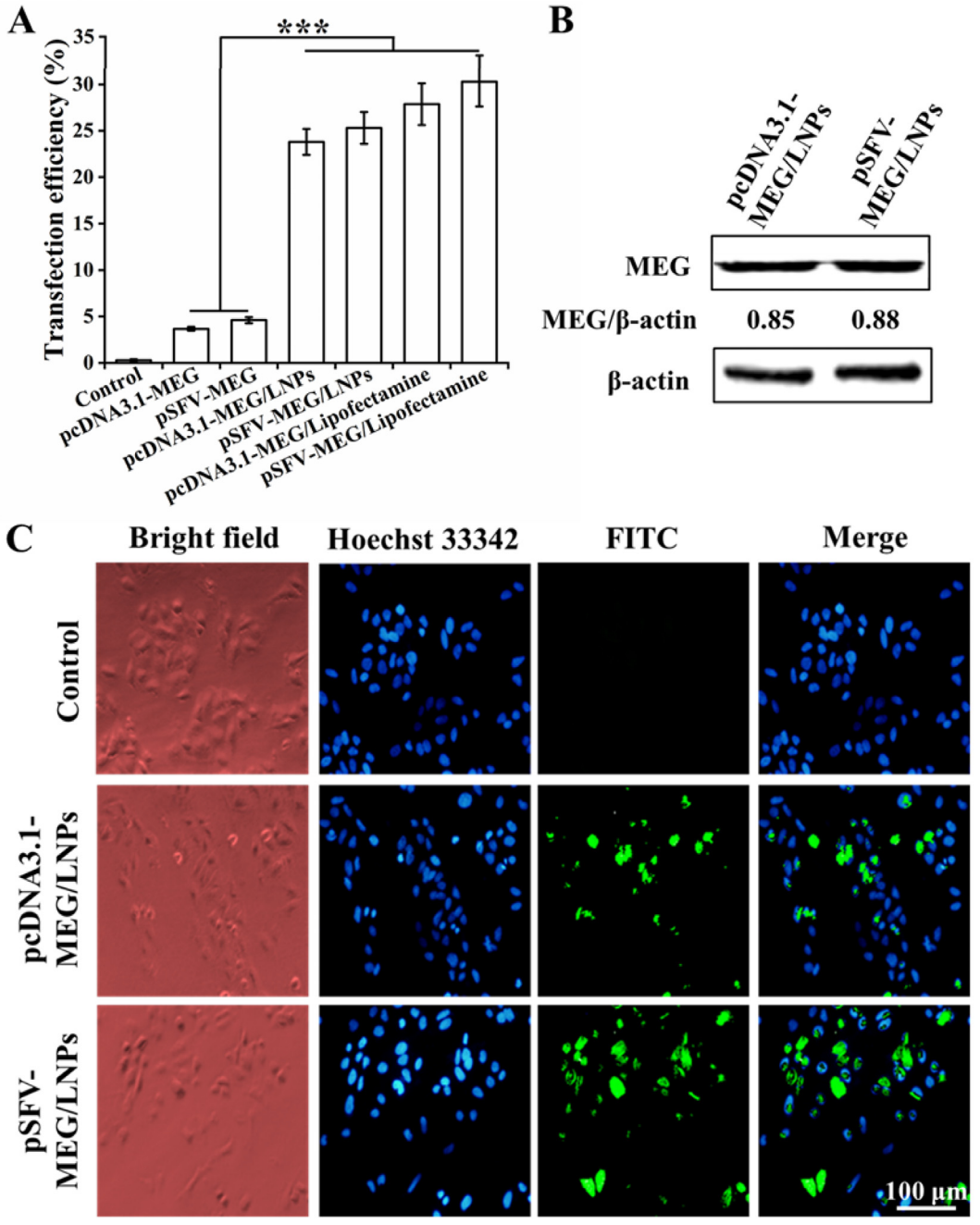

Figure 7. Antigen expression in L-02 cells. **(A)** Transfection efficiency of pcDNA3.1-MEG, pSFV-MEG, pcDNA3.1-MEG/LNPs, pSFV-MEG/LNPs, pcDNA3.1-MEG/Lipofectamine, and pSFV-MEG/Lipofectamine. Data were expressed as mean ± SD (n = 3). *$P < 0.05$, **$P < 0.01$, and ***$P < 0.001$. **(B)** The expression of MEG antigen in L-02 cells measured by western blotting. **(C)** The expression of MEG antigen in L-02 cells was detected by immunofluorescence analysis. Green and blue colors indicate anti-His antibody conjuncted FITC and Hoechst 33342, respectively. Bar = 100 μm.

successfully developed as a drug delivery system with PLGA core.[48,49] Herein, we developed a novel LNPs with an mPEG-PLGA core and a shell made of lecithin and DSPE-PEG-Mal 2000. The mostly used DNA delivery strategies are physical methods, such as electroporation, DNA tattooing, jet injectors, and gene gun, which are able to overcome the multi-barrier to transport DNA into the nucleus, but it can cause cell damage and discomfort at the injection site.[8] Muscle cells were demonstrated to be the only cells observed to translate the directly-injected plasmid DNA into protein.[11] The accumulatively release of DNA from LNPs was 51.11% at 96 h in this study, which played a good sustained release effect because plasmid DNA had been detected to persist in muscle up to 6 months in a non-integrated fashion.[11] The encapsulation efficiency of pSFV-MEG/LNPs (87.60 ± 8.73%) prepared was higher than that of Zhang et al. (59 ± 4%),[24] which was attributed to mPEG-modification that improved the stability of DNA and polymers in an organic solvent.[46] In the current study, the developed LNPs had a

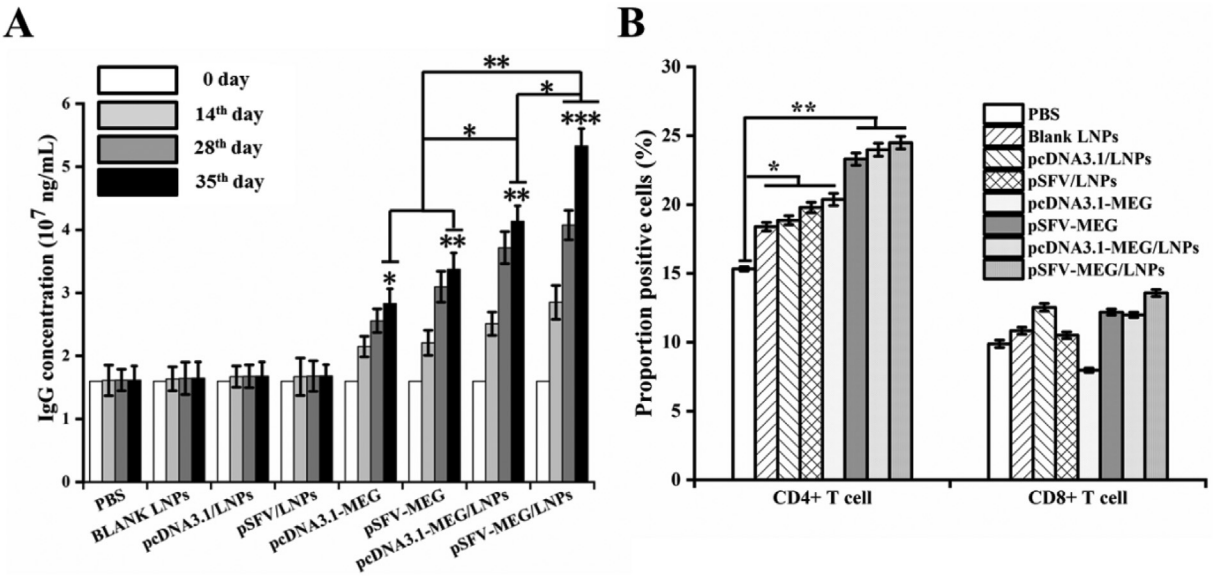

Figure 8. Induction of anti-MEG humoral and cellular responses in mice vaccinated with pSFV-MEG/LNPs. **(A)** Levels of total serum anti-MEG IgG. Mice were intramuscular vaccinated 3 times at 2-week intervals with PBS, blank LNPs, pcDNA3.1/LNPs, pSFV/LNPs, pcDNA3.1-MEG/LNPs, and pSFV-MEG/LNPs. Serum samples were then collected on day 0, 14, 28, and 35 after the primary, secondary, and third vaccination. **(B)** The proportion of CD4+ T and CD8+ T cells in the spleen was analyzed by flow cytometry. Splenocytes from three mice in each group after the third immunization were stained with mouse anti-CD4 and anti-CD8 monoclonal antibodies. Data were expressed as mean ± SD (n = 3). * $P < 0.05$, ** $P < 0.01$, and *** $P < 0.001$.

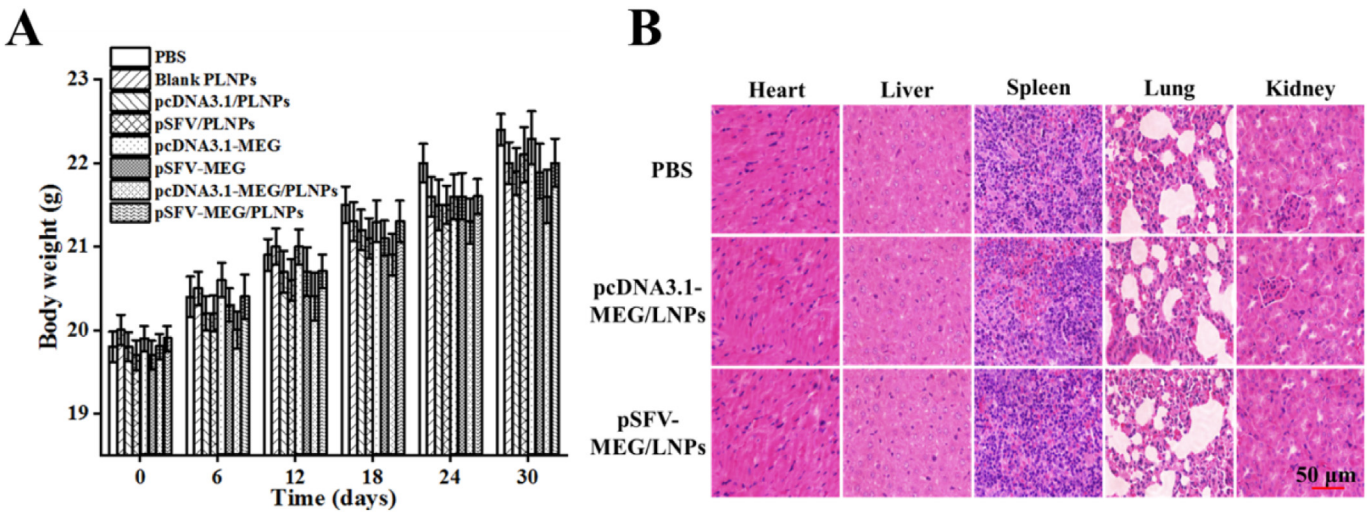

Figure 9. Changes of body weights and HE staining of the main organs of the mice. **(A)** The body weight of mice was measured every 3 days. Data were expressed as mean ± SD (n = 3). **(B)** HE staining was used to observe the morphology of the main organs of mice after the third immunization. All images were taken at 400× magnification. Bar = 50 μm.

particle size of 161.61 ± 15.63 nm, which might provide protection against RES clearance. NPs with a particle size more than 200 nm are quickly cleared by the liver and spleen, while in 50–100 nm are readily accumulation in liver, less than 5 nm will be filtered by the kidney.[50,51] Besides, the LNPs had negligible toxicity against cells because of mPEG-PLGA was a FDA-approval polymer and lecithin was a natural lipid extracted from soybean, as reported previously. [43,52] Furthermore, the pSFV-MEG/LNPs induced a better humoral (1.58-fold) and $CD4^+$ T cells immunity (1.05-fold) compared to pSFV-MEG. The results suggested that LNPs could enhance the immune responses. However, the pSFV-MEG/LNPs did not induce $CD8^+$ T cells response, which may be due to $CD4^+$ T cells were essential for inducing B cell responses and maintaining its long-term immunological memory in bacteria and parasite infectious, while $CD8^+$ T cell response played a central role in intracellular viral infections and cancer.[33,34] Besides, the prepared LNPs had a negative zeta potential (−17.5 ± 0.5 mV and − 29.3 ± 0.3 mV for blank LNPs and pSFV-MEG/LNPs, respectively) (Table 3), which might affect the uptake rate of the LNPs by cells. If the

surface of the LNPs were further modified to a positive zeta potential, it could greatly increase the uptake of the LNPs by cells and enhance the immune response.

According to the experimental results, the usage of self-replicating multi-epitope DNA vaccine as a new generation vaccine and LNPs as a new delivery system should be proposed. As a result, after change the antigen it was used in the prevention and treatment of other diseases, such as ZIKA virus (ZIKV), Ebola virus (EBOV), the coronaviruses-Middle East respiratory syndrome coronavirus (MERS-CoV), and even the COVID-19. In addition, the LNPs without toxicity protected the DNA from the degradation of DNase perfectly, improved the transfection efficiency, and released DNA slowly to achieve sustained antigenic stimulation. Moreover, the rationally designed DNA vaccine encapsulated in LNPs could stimulate a better humoral and cellular immunity compared to the blank ones. Furthermore, the pSFV vector and LNPs enhanced the immune response to a degree. Most importantly, the immune efficiency of the multi-epitope DNA vaccine could be further improved by optimizing the NPs to reduce the sudden release and co-administration with a suitable adjuvant.

Conclusion

In this study, we have successfully developed a novel biodegradable LNPs to protect and deliver the immunogenic DNA vaccine (pSFV-MEG/LNPs). The tertiary structure of MEG antigen was sable. Besides, 58.5% residues of MEG had a high antigen index close to 1.7. Moreover, the LNPs together with pSFV vector enhanced the immune response of MEG. After immunization, pSFV-MEG/LNPs performed stronger humoral (3.22-fold) and cellular immune (1.60-fold) responses compared with PBS group. In summary, we have successfully developed a new DNA vaccine and nano-delivery system, providing a novel type of vaccine strategy for the treatment and prevention of other bacterial and viral infectious diseases.

Appendix A. Supplementary data

Supplementary data to this article can be found online at https://doi.org/10.1016/j.nano.2020.102338.

References

1. The top 10 causes of death [EB/OL]. (2018-05-24) [2020-05-25]. https://www.who.int/en/news-room/fact-sheets/detail/the-top-10-causes-of-death.
2. Coronavirus disease (COVID-19) pandemic [EB/OL]. (2020-05-25) [2020-05-25]. https://www.who.int/emergencies/diseases/novel-coronavirus-2019.
3. Vanessa C, King CE, Kalan L, Mora M, Sung WWL, Schwarz C, et al. Antibiotic resistance is ancient. *Nature* 2011;**477**:457-61.
4. Lewis K. *The Science of Antibiotic Discovery Cell* 2020;**181**:29-45.
5. Hobernik D. DNA vaccines-how far from clinical use? *Int J Mol Sci* 2018;**19**:3605.
6. Lim M, Firdous J, Azad M, Mannan A, Al-Hilal TA, Cho CS, et al. Engineered nanodelivery systems to improve DNA vaccine technologies. *Pharmaceutics* 2020;**12**:30.
7. Zhang M, Chen W, Wang C. Polymers for DNA vaccine delivery. *ACS Biomater Sci Eng* 2017;**3**:108-25.
8. Lopes A, Préat V. Cancer DNA vaccines: current preclinical and clinical developments and future perspectives. *J Exp Clin Cancer Res* 2019;**38**:146.
9. Farris E, Ramer-Tait AE, Pannier AK. Micro- and nanoparticulates for DNA vaccine delivery. *Exp Biol Med* 2016;**241**:919-29.
10. Flingai S, Goodman J, Kudchodkar SB, Muthumani K, Weiner DB. Synthetic DNA vaccines: improved vaccine potency by electroporation and co-delivered genetic adjuvants. *Front Immunol* 2013;**4**:354.
11. Liu MA. A comparison of plasmid DNA and mRNA as vaccine technologies. *Vaccine* 2019;**7**:37.
12. Gummow J, Mekonnen ZA, Li Y, Wijesundara DK, Shrestha AC, Voskoboinik L, et al. Safety profile of a multi-antigenic DNA vaccine against hepatitis C virus. *Vaccine* 2020;**8**:1-15.
13. Pang J, Wang MX, Ang IYH, Tan SHX, Lewis RF, Chen JIP, et al. Potential rapid diagnostics, vaccine and therapeutics for 2019 novel coronavirus (2019-nCoV): a systematic review. *J Clin Med* 2020;**9**.
14. Scancell to initiate development of novel DNA vaccine against COVID-19 [EB/OL]. (2020-04-24) [2020-05-25]. https://www.scancell.co.uk/development-of-vaccine-against-covid-19. 2020.
15. Inovio's COVID-19 DNA vaccine INO-4800 demonstrates robust neutralizing antibody and T cell immune responses in preclinical models [EB/OL]. (2020-05-20) [2020-05-25]. http://ir.inovio.com/news-releases/news-releases-details/2020/INOVIOs-COVID-19-DNA-Vaccine-INO-4800-Demonstrates-Robust-Neutralizing-Antibody-and-T-Cell-Immune-Responses-in-Preclinical-Models/default.aspx. 2020.
16. CanSinoBio's investigational vaccine against COVID-19 approved for phase 1 clinical trial in China [EB/OL]. (2020-05-17) [2020-05-25]. http://www.cansinotech.com/homes/article/show/56/153.html. 2020.
17. Gary EN, Weiner DB. DNA vaccines: prime time is now. *Curr Opin Immunol* 2020;**65**:21-7.
18. Harro C, Bourgeois AL, Walker R, DeNearing B, Feller A, Chakraborty S, et al. A combination vaccine consisting of three live attenuated enterotoxigenic *Escherichia coli* strains expressing a range of colonization factors and heat-labile toxin subunit B is well tolerated and immunogenic in a placebo-controlled double-blind phase I trial in healthy adults. *Clin Vaccine Immunol* 2011;**18**:2118-27.
19. Fleckenstein JM, Qadri F. Novel antigens for enterotoxigenic *Escherichia coli* vaccines. *Expert Rev Vaccines* 2014;**13**:631-9.
20. Croxen MA, Scholz R, Keeney KM, Wlodarska M, Finlay BB. Recent advances in understanding enteric pathogenic Escherichia coli. *Clin Microbiol Rev* 2013;**26**:822-80.
21. Roehrich D, Johnson S, Blocker AJ, Veenendaal AKJ. The extreme C terminus of Shigella flexneri IpaB is required for regulation of type III secretion, needle tip composition, and binding. *Infect Immun* 2010;**78**:1682-91.
22. Cao A, Wang J, Li X, Wang S, Zhao Q, Cong H, et al. Toxoplasma gondii: vaccination with a DNA vaccine encoding T- and B-cell epitopes of SAG1, GRA2, GRA7 and ROP16 elicits protection against acute toxoplasmosis in mice. *Vaccine* 2015;**33**:6757-62.
23. Cao Y, Fu Y, Bai Q, Chen Y, Bai X, Jing Z, et al. Rational design and efficacy of a multi-epitope recombinant protein vaccine against foot-and-mouth disease virus serotype a in pigs. *Antiviral Res* 2017;**140**:133-41.
24. Zhang L, Gu FX, Rhee JW, Wang AZ, Radovic-Moreno AF, Alexis F, et al. Omid C Farokhzad, self-assembled lipid–polymer hybrid nanoparticles: a robust drug delivery platform. *ACS Nano* 2008;**2**:1696-702.
25. Khatoon N, Prajapati VK. Exploring Leishmania secretory proteins to design B and T cell multi-epitope subunit vaccine using immunoinformatics approach. *Sci Rep* 2017;**7**:8285.
26. Pandey RK, Prajapati VK. Novel immunoinformatics approaches to design multi-epitope subunit vaccine for malaria by investigating anopheles salivary protein. *Sci Rep* 2018;**8**:1125.

27. Chauhan V. Immuno-informatics approach to design a multi-epitope vaccine to combat cytomegalovirus infection. *Eur J Pharm Sci* 2020;**147**:105279.
28. Chen X, Shen WC. Fusion protein linkers: property, design and functionality. *Adv Drug Deliv Rev* 2013;**65**:1357-69.
29. Yanoa A, Asahi-Ozaki Y, Imai S, Hanada N, Miwa Y, Nisizawa T. An ingenious design for peptide vaccines. *Vaccine* 2005;**23**:2322-6.
30. Kreiter S, Diken M, Sebastian M, Osterloh P, Schild H, Huber C, et al. Ugur Sahin, increased antigen presentation ffficiency by coupling antigens to MHC class I trafficking signals. *The Journal of Immunology* 2008;**180**:309-18.
31. Dunn SS, Parrott MC. Zapped assembly of polymeric (ZAP) nanoparticles for anti-cancer drug delivery. *Nanoscale* 2019;**11**:1847-55.
32. Serradell MC, Martino RA, Prucca CG, Carranza PG, Saura A, Fernández EA, et al. Efficient oral vaccination by bioengineering virus-like particles with protozoan surface proteins. *Nat Commun* 2019;**10**.
33. Simerska P, Ziora ZM, Rivera FDL, Engwerda C, Toth I. Ovalbumin lipid core peptide vaccines and their CD4(+) and CD8(+) T cell responses. *Vaccine* 2014;**32**:4743-50.
34. Shu J, Liu H, Jin X, Xu J. The immunologic dominance of an epitope within a rationally designed poly-epitope vaccine is influenced by multiple factors. *Vaccine* 2020;**38**:2913-24.
35. Steffen R, Steffen R, Hill DR, Dupont HL. Traveler's diarrhea: a clinical review. *JAMA* 2015;**313**:71-80.
36. Kotloff KL, Blackwelder WC, Nasrin D, Farag TH, Panchalingam S, Wu Y, et al. Burden and aetiology of diarrhoeal disease in infants and young children in developing countries (the global enteric multicenter study, GEMS): a prospective, case-control study. *The Lancet* 2013;**382**:209-22.
37. Yuan Y, Xu X, Liu Y, Li C, Yang M, Yang Y, et al. Evaluation of a dual-acting antibacterial agent, TNP-2092, on gut microbiota and potential application in the treatment of gastrointestinal and liver disorders. *ACS Infect Dis* 2020;**5**:820-31.
38. Albert ML, Bhardwaj N. Dendritic cells acquire antigen from apoptotic cells and induce class I-restricted CTLs. *Nature* 1998;**392**:86-9.
39. Heine SJ, Chen X, Choudhari S, Blackwelder WC, Roosmalen MLV, Leenhouts K, et al. Shigella IpaB and IpaD displayed on L. lactis bacterium-like particles induce protective immunity in adult and infant mice. *Immunol Cell Biol* 2015;**97**:641-52.
40. Chen X, Martinez-Becerra FJ, Kim JH, Dickenson NE, Toth IV RT, Joshi SB, et al. Impact of detergent on biophysical properties and immune response of the IpaDB fusion protein, a candidate subunit vaccine against Shigella species. *Infect Immun* 2015;**83**:292-9.
41. Chakraborty S, Vickers TJ, Molina D, Harro CD, DeNearing B, Brubaker J, et al. Interrogation of a live-attenuated enterotoxigenic Escherichia coli vaccine highlights features unique to wild-type infection. *NPJ Vaccines* 2019;**4**:37.
42. MM, Aminianfar M, Moghaddam G, Nematollahi A. A multi-method and structure-based in silico vaccine designing against Echinococcus granulosus through investigating enolase protein. Bioimpacts 2019;9:131–440.
43. Lu Y, Duan W, Mu X, Fang S, Lu N, Zhou X, et al. Engineering a "PEG-g-PEI/DNA nanoparticle-in- PLGA microsphere" hybrid controlled release system to enhance immunogenicity of DNA vaccine. *Materials Science & Engineering C* 2020;**106**:110294.
44. Shae D, Wilson JT. Vaccine delivery: where polymer chemistry meets immunology. *Future Science* 2016;**7**:193-6.
45. Buschmann∗ MD, Lavertu M, Thibault M, Jean M, Darras V. Chitosans for delivery of nucleic acids. Adv Drug Deliv Rev 2013;65:1234–70.
46. Harris M. Effect of pegylation on pharmaceuticals. *Nat Rev Drug Discov* 2003;**2**:214-21.
47. Kolate A, Patil S, Vhora I, Kore G, Misra A. PEG - a versatile conjugating ligand for drugs and drug delivery systems. *J Control Release* 2014;**192**:67-81.
48. Dehaini D, Pang Z, Hu CMJ, Kroll AV, Yu CL, Gaoa W, et al. Ultra-small lipid–polymer hybrid nanoparticles for tumor-penetrating drug delivery. *Nanoscale* 2016;**8**:14411-9.
49. Wu B, Zhang LJ, Zhuo RX, Xu HB, Huang S. Codelivery of doxorubicin and triptolide with reduction-sensitive lipid-polymer hybrid nanoparticles for in vitro and in vivo synergistic cancer treatment. *Int J Nanomedicine* 2017;**12**:1853-62.
50. Nguyen DN, Chan JM, Langer R, Anderson DG. Polymeric materials for gene delivery and DNA vaccination. *Adv Mater* 2009;**21**:847-67.
51. Hu F, Yan T, Guo W, Liu Q, Han M, Liu C, et al. Multiple targeting strategies achieve novel protein drug deliver into cancer cells to proapoptosis lung cancer cell by precisely inhibiting survivin. Nanoscale 2020;12:10623–138.
52. Song Y, Hurk SVDLVD, Chen L. Cellulose-based polyelectrolyte complex nanoparticles for DNA vaccine delivery. *Biomater Sci* 2014;**2**:1440-9.